International Journal of Modern Manufacturing Technologies
ISSN 2067–3604, Vol. XVI, No. 1 / 2024
https://doi.org/ 10.54684/ijmmt.2023.16.1.141

NUMERICAL SIMULATIONS OF ELASTIC-PLASTIC CONTACT CONSIDERING FRICTION

Sergiu Spinu[1,2]

[1] Department of Mechanics and Technologies, Stefan cel Mare University of Suceava,
13th University Street, 720229, Romania
[2] Integrated Center for Research, Development and Innovation in Advanced Materials, Nanotechnologies, and Distributed Systems for Fabrication and Control (MANSiD), Stefan cel Mare University, Suceava, Romania

Corresponding author: Sergiu Spinu, sergiu.spinu@fim.usv.ro

Abstract: The solution of the elastic-plastic contact is of major importance in contact mechanics because contact damage and wear are responsible for the failure of many machine elements subjected to contact load. In many situations including gears and bearings, the load is transmitted through a small contact region, i.e. a concentrated contact, and the resulting high gradients of stress often exceed the plastic yield limit of the softer material. Plastic flow is initiated at a certain depth, resulting in modification of contact geometry and of the stress state that can lead to crack inception and propagation. Understanding the contact behaviour in the presence of plastic strains is fundamental for predicting the contact resistance. Considering the mathematical model complexity for the contact between bodies of arbitrary boundary, as well as the dissipative nature of plasticity, an analytical solution for the elastic plastic contact problem is hard to accomplish. Alongside finite element analysis, semi-analytical methods are the only existing simulation tools for the elastic-plastic contact problems. This paper extends a previously reported elastic-plastic contact solver developed by the same author, by considering friction. In the previous solver iteration, residual displacements were calculated only in the normal contact direction, thus assuming that the shear displacements are small enough to be neglected, in other words, the contact was assumed frictionless. By considering friction, a slip-stick contact process is introduced, adding a new iterative loop in which the contact pressure and shear stresses are iterated until convergence is reached. The new computer simulation tool is expected to give more realistic predictions for the elastic-plastic contact between materials with dissimilar elastic properties, in which case the shear tractions disturb the stress and displacements fields calculated for the frictionless contact case. The results are expected to contribute to a better understanding of the contact processes in the presence of both plastic strains and friction.

Key words: elastic-plastic contact, friction, semi-analytical method, repeated contact, rolling.

1. INTRODUCTION

Both plasticity and contact mechanics require numerical analysis to achieve solutions of practical applicability. The few cases of analytical solutions in contact mechanics involve purely elastic behavior of the contacting materials, and axisymmetric contact geometry [1]. When friction is also accounted for in a slip-stick contact scenario, closed form solutions were achieved only for similar elastic materials, e.g. the solution of the Cattaneo-Mindlin problem, cited in [1]. Consideration of plasticity in contact mechanics adds the need for the reproduction of the loading history, which is also required to replicate the influence of friction when the contacting materials have different constitutive laws. Thus, numerical analysis with discretization of both the spatial domain and the loading curve is required to obtain an elastic-plastic frictional contact solution. Whereas finite element analysis (FEA) fulfils these requirements [2,3], is may not be the best course of action for non-conforming contact such as those appearing in gears or bearings. In these cases, steep gradients are highly localized in a vicinity of the initial point of contact, whereas the meshing of the entire bulk, as required by FEA, increases the computational time beyond reasonable limits even when adaptive meshes are imposed.
To overcome this limitation, researchers in contact mechanics have developed an alternative numerical approach based on fundamental solutions for the elastic-half-space. In this framework, by regarding the contacting bodies as half-spaces, solutions can be achieved with the discretization of a limited region neighboring the region of interest, i.e. the initial point of contact. Solutions for the normal elastic-plastic contact were thus obtained [4-8] with much less computational effort compared to FEA efforts. The tangential effects related to friction were also considered [9-11], but mostly the simpler case of full sliding, in which the interdependence between the normal and the tangential contact problems is not accounted for.

In most situations, a contact is first loaded in the normal direction, and a subsequent tangential load, i.e. a tangential force or a twisting moment, are applied. Whereas full sliding is likely to occur in this second stage of simultaneous normal and tangential loading, in the first stage of normal load, sliding will take place on a limited region of the contact area, e.g. on a peripheral ring encircling a central stick region as shown by the Cattaneo-Mindlin solution. Therefore, in slip-stick contact is a more complex case because the its full-sliding counterpart, because multiple iterative levels are required to derive not only the contact area, but also the stick area and the distribution of shear tractions on it. Moreover, there exist multiple dependencies between the problem parameters: contact pressure induces tangential displacements affecting the shear traction, while the latter generates normal displacements that modify the interference equation in the normal direction. For these reasons, an analytical solution to the slip-stick contact, even in the less complex elastic domain, has yet to emerge, and little information on the elastic-plastic slip-stick contact exists in the literature. These authors [12] proposed an efficient solution to the contact problem under the assumption of partial slip at the boundary of an elastic-plastic body. The numerical simulations indicated that the progression of slip was influenced by the plastic strains, and the contact tractions exhibited a more complex behavior compared to their elastic counterparts.
This paper tackles the frictional elastic-plastic contact by extending a previous contact code by the same author, in which the algorithm sequence charged with the finding of contact pressure is replaced by a two-level nested loop which finds the contact pressure and the shear tractions, thus simulating a slip-stick contact process.

2. ALGORITHM ENHANCEMENTS

An algorithm for the simulation of the elastic-plastic contact was proposed in a previous effort [13], organised on three nested loops:

1. The outer loop replicates the loading history, which is mandatory considering that plasticity is a dissipative process. In problems involving plasticity, the final state cannot be evaluated without the simulation of all intermediate states.
2. The middle-level loop, also called the elastic loop, derives the solution of the contact problem for arbitrary contact geometry. The latter solution is attained based on the assessment of displacement as the sum of two contributions: (a) the displacement due to pressure, calculated by superposition of solutions for point forces acting on the boundary of an elastic half-space, and (b) the displacement due to the plastic strains, detailed in [14]. It should be noted that (a) is the recoverable displacement component, which vanishes if the load is removed, whereas (b) is a permanent (residual) part. The latter is also referred as the residual print.
3. The innermost loop computes the increment of plastic strains by numerical resolution of the equation describing the surface of plastic flow via Newton-Raphson iteration.

The novelty of this paper is the enhancement of the intermediate loop with the tangential effects. In the previously reported efforts [13], only the normal contact problem was solved. This can be a reasonable simplification when there exist little to no friction between the contacting surfaces, or when corresponding points on the contacting surfaces undergo similar tangential displacements. Considering that the displacement is the sum of two independent contributions, the latter condition is unlikely to be met for arbitrary materials. Thus, if friction exist, the different deformation of surfaces in the tangential direction will give birth to shear traction. The latter are the source of normal displacements that eventually disturb the contact pressure. Thus, there exists a mutual interaction between contact pressure and shear tractions, which must be accounted for when either of the following conditions are met: (a) the frictional coefficient between the contacting surfaces is high, (b) the contacting materials are very dissimilar with respect to their elastic parameters, and (c) when the tangential residual displacements due to the plastic strains are of the same order of magnitude as the ones due to pressure.
The integration of the tangential effects in the existing elastic-plastic contact code is supported by the following results:

1. The tangential displacement due to arbitrary distributions of plastic strains can be calculated [14].
2. The contact problem with consideration of both normal and tangential directions can be solved under the assumption of a slip-stick regime for arbitrary contact geometry [15].

In the newly developed code presented in this work, the intermediate loop is replaced with a two-level nested loop charged with the solution of the slip-stick contact problem for random contact geometry. Essentially, the one-level iteration for the solution of the normal contact problem, i.e. the middle loop, is replaced with the two-level nested loop proposed in [15] for the slip-stick contact, resulting in a 4-level nested loop algorithm structure.
The flow chart for the enhanced algorithm is outlined in figure 1. A detailed description of various algorithm steps is beyond the goal of this paper, but can be compiled from different sources [4, 13-15].

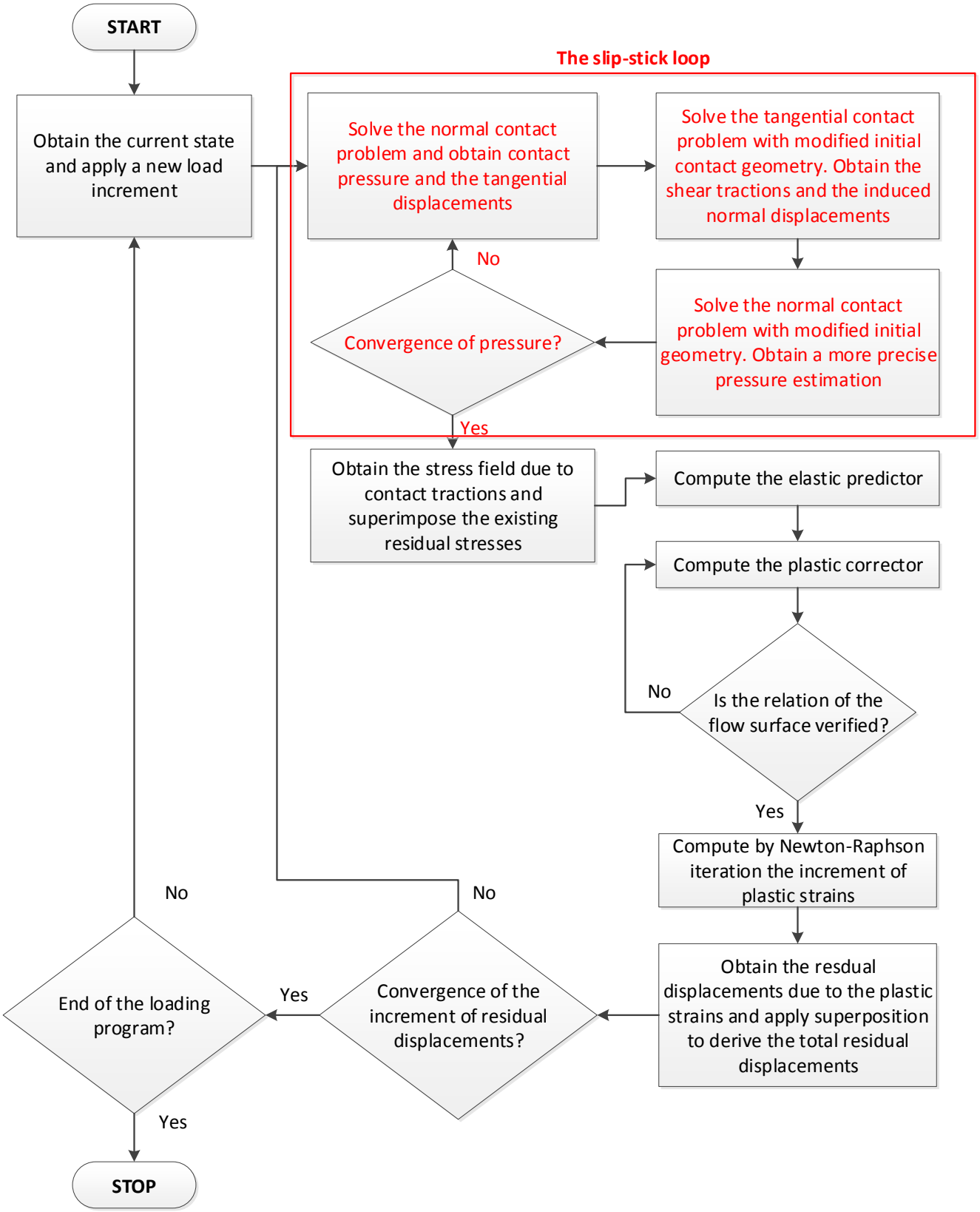

Fig. 1. Flow-chart of the algorithm for the simulation of the elastic-plastic contact with friction

The algorithm follows the approach described in [13], except for the intermediate (or elastic) loop, which is replaced by a slip-stick loop aiming to solve the problem of the contact with slip and stick on the contact area. The latter loop involves successive solutions of the normal and of the tangential contact problems, until pressure varies from one iteration to the next within an imposed precision. Either normal or the tangential solutions are based on the Conjugate Gradient method. As shown in [15], a master scheme can solve both the normal and the tangential contact problem. This iterative process is required as the normal and tangential contact problems are

not independent: contact pressure induces tangential displacements that affect or generate shear tractions, whereas shear tractions in their turn induce normal displacements that influence the contact pressure. Moreover, in the slip regions of the contact area, contact pressure and shear tractions are related through Hooke's law of friction. The intensity of this interaction between the normal and the tangential effects is estimated by the so-called Dundurs parameter:

$$\beta = \frac{(1+\nu_1)(1-2\nu_1)/(2E_1) - (1+\nu_2)(1-2\nu_2)/(2E_2)}{(1-\nu_1^2)/E_1 + (1-\nu_2^2)/E_2}, \quad (1)$$

in which E_i and ν_i are the elastic parameters, i.e. the Young modulus and the Poisson's ratio of the body *i*,
This model assumes that the both slip and stick occurs on the contact area, which is a more general case than full sliding, in which no stick is allowed and the shear tractions are simply the product of pressure and the frictional coefficient. The latter case was considered in [10].

3. ELASTIC-PLASTIC CONTACT WITH GEOMETRIC SYMMETRY

Considering that a distribution of subsurface plastic strain results in permanent displacement of the free surface points, both along normal and tangential direction, a rigorous solution for the contact problem cannot be achieved based on the interference equation along the normal direction alone. The latter approach is taken in many papers [4-8], and implies that the shear contact tractions and displacements have little or no influence on the contact process. The latter is true if friction is not accounted for, but otherwise an interference equation in the tangential direction should also be solved. Indeed, if the tangential displacements of corresponding points are different, either induced by contact pressure of by the plastic volume, the relative displacement will be resisted by friction, leading to the development of shear traction. The latter will in their turn affect the contact in the normal direction, thus perturbing the interference equation in the normal direction. Consequently, when friction is accounted for in the contact problem, the contact problem involves interference equations in the directions both normal and tangential. One exception from the latter rule can be formulated for the purely elastic contact, namely the case of similarly elastic contacting materials. In this scenario, the identical pressure acting on both contacting bodies will generate perfectly matched tangential displacements of discrete points from the two contacting surfaces. In other words, the deformed surfaces will comply in the tangential direction, and even if friction exist, no shear tractions are generated. It follows that, in the case of the contact between similarly elastic materials that can be approximated with elastic half-spaces, the exact problem solution can be achieved with a problem model for the normal direction alone.
The problem is more complicated in the elastic-plastic case, because the displacement has two components, the one due to contact pressure and the other due to the plastic strains. In order to achieve the aforementioned condition in which shear tractions are not generated during contact loading/unloading, the displacement component due to the plastic volume must also be identical, so that the sum of the two can be perfectly matched all over the contact area. The latter condition is satisfied under two restrictions: (1) the initial contact geometry is symmetrical about the common plane of contact (e.g. the contact between identical spheres), and (2) the same elastic properties and the same hardening law are presumed for both contacting materials. Under these assumptions, the plastic volumes emerging in the two contacting bodies are also symmetrical about the common plane of contact, resulting in identical residual displacements that do not further disturb the contact process along the normal direction. Consequently, a contact study on the normal direction alone yields the correct solution even when friction is present. Compared to the contact code for the frictionless contact, the algorithm remains the same except for the interference equation along the normal direction, in which the total displacement is double the displacement calculated for one body. It follows that the development of plastic strains must be monitored only for one of the two contacting bodies. The new interference equation becomes:

$$h \leftarrow hi + 2(u_3^r + u_3^p) - \delta, \quad (2)$$

in which u_3^r is the residual component of displacement, and u_3^p the component due to contact pressure, which is recovered after unloading. Equation (2) preserves the algorithm structure and allows for the direct application of the algorithm for the frictionless contact [13] to the frictional elastic-plastic contact with geometric symmetry and identical elastic properties and hardening law.
A series of contact simulations were performed by implementing this idea to a sphere-on-sphere contact with

friction. The assumed behaviour of the contacting materials includes purely elastic (E) and elastic-plastic isotropic hardening (EP) described by Swift's power law. The input data concerning the contacting bodies is depicted in table 1.

Table 1. Description of the contacting bodies

	Undeformed contact geometry	Behavior	Elastic parameters	Plastic parameters (isotropic hardening law)
body 1	Sphere with radius $R=0.015m$	E	$E_1=210GPa$, $\nu_1=0.3$	-
		EP	$E_1=210GPa$, $\nu_1=0.3$	Swift's law with $B_1=945MPa$, $C_1=20$, $n_1=0.121$
body 2	Sphere with radius $R=0.015m$	E	$E_2=210GPa$, $\nu_2=0.3$	-
		EP	$E_2=210GPa$, $\nu_2=0.3$	Swift's law with $B_2=945MPa$, $C_2=20$, $n_2=0.121$

B_i C_i and n_i, are the parameters for the body i entering the Swift's law giving the increase of the elastic domain of the material subjected to load that surpasses its elastic limit:

$$\sigma_Y(e^p)=B(C+10^6e^p)^n. \tag{3}$$

The latter suggests that the plastic yield limit σ_Y of the material increases with the development of new equivalent plastic strains e^p. The assumed expansion of the elastic domain is effective even when the load changes its sign, thus describing an isotropic hardening law, as opposed to kinematic hardening, in which the increase is apparent only for a load of the same sign.

The contact between the bodies described in table 1 was loaded up to a normal force of $W=11179\ N$. The Hertz purely elastic model (E-E) predicts a hertzian central pressure $p_H=8GPa$ and a contact radius $a_H=817\,\mu m$. The predictions of the simulation program for the contact case EP-EP (both bodies elastic-plastic) are depicted in figures 2-4. The contact case E-EP, i.e. one body elastic and the other one elastic-plastic, is also added for comparison, although its predictions are not expected to be accurate, because of influence of the tangential residual displacements that have no match on the elastic body, which is not accounted for. However, this approach for the E-EP contact without a study of the tangential effect is taken in many studies. Figure 3 depicts the radial profiles of dimensionless pressure for the three contact cases, at the end of the loading program, i.e. when $W=11179\ N$. Compared to the elastic case, the elastic-plastic pressure is flattened when an elastic-plastic behaviour is assumed.

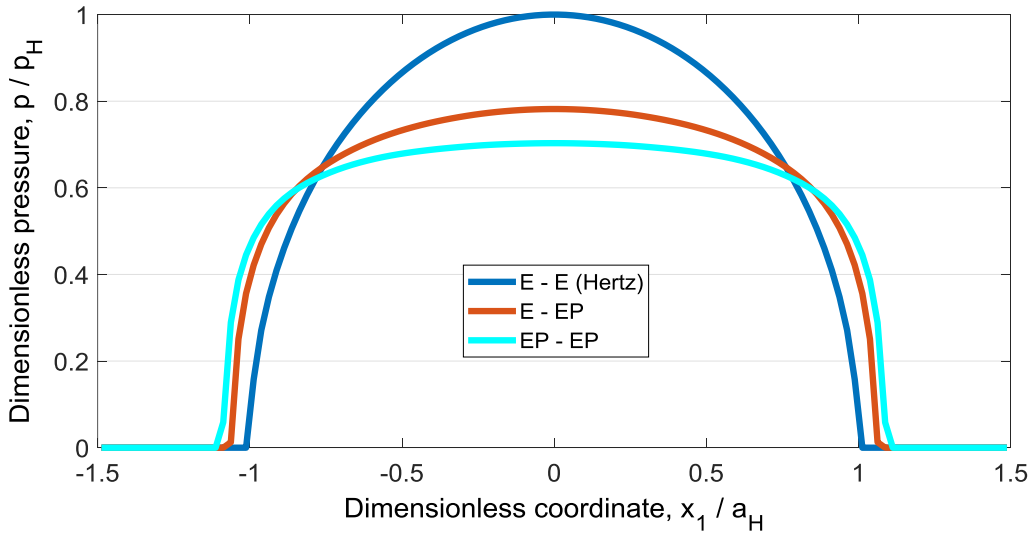

Fig. 2. Dimensionless pressure for various contact cases at maximum load

It should be remembered that, in order to obtain an elastic-plastic solution, the history of the loading process must be simulated by incremental load application. This allows the depiction of the history of the maximum central pressure (figure 2) and of the accumulated plastic strain (figure 3) with the load level. One can see that the higher pressure maximums in the E-EP case translates to plastic strains compared to the EP-EP case.
In these specific contact cases, the contact process can thus be simulated by neglecting friction without significant errors. On the other hand, the next section presents a contact situation in which the solution cannot be obtained and explained without studying the contact process in the tangential direction along the normal one.

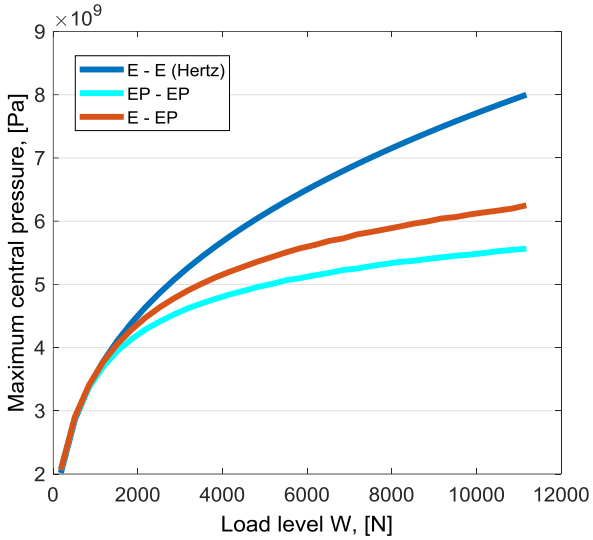

Fig. 3. Maximum pressure vs. load level

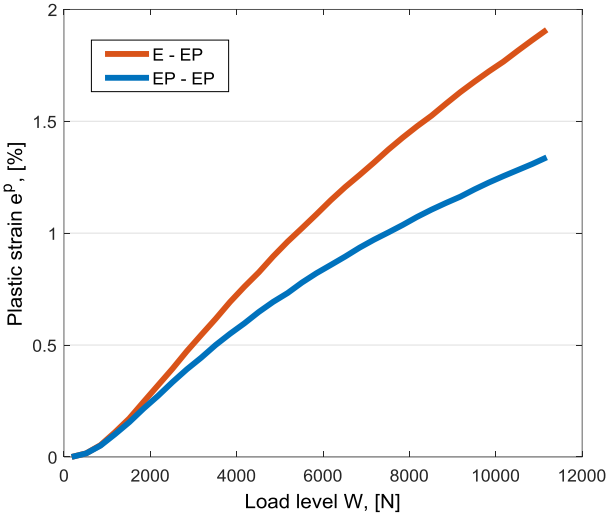

Fig. 4. Plastic strain vs. load level

4. SIMULATION OF FRETTING TYPE II

Fretting is one of the major causes of failure of machine elements due to small tangential oscillations resulting from vibrations during the service life of the product. The type I fretting appears when a tangential load is explicitly applied after the contact is established, whereas the type II is specific to pure normal loading. In the latter case however, although a tangential force is not applied, there exist shear contact stresses related to the discrepancy in the properties of the contacting materials. Thus, when friction is considered, the contact problem in the tangential direction must be considered and solved even when no tangential force is explicitly applied. Furthermore, the interaction between the contact problems in the tangential and in the normal direction must be considered, because the shear tractions perturb the contact pressure, whereas the latter affects the shear tractions according to the Hooke's law of friction. This mutual interaction can be simulated with the enhancements of the frictionless elastic-plastic contact code proposed in this paper.
The simulated contact involves the indentation of an elastic-plastic half-space with isotropic hardening by a rigid spherical indenter, as shown in table 2. The contact is loaded with a normal force applied in small increments, until a maximum value that, according to the Hertz purely elastic model, would generate a $p_H = 6GPa$ central pressure. A rectangular domain of side lengths $[-1.5a_H;1.5a_H]\times[-1.5a_H;1.5a_H]\times[0;1.2a_H]$ is discretised with a $64\times64\times64$ uniform mesh. The friction coefficient μ is varied to assess the influence of the friction intensity on various contact parameters. Figure 5 depicts the dimensionless contact tractions predicted for the maximum load, for usual values of the frictional coefficient between metallic materials. The Hertz contact parameters p_H and a_H were used as normalizers.

Table 2. Description of the contacting bodies for the fretting simulation

	Undeformed contact geometry	Behavior	Elastic parameters	Plastic parameters (isotropic hardening law)
body 1	Sphere with radius $R = 0.015m$	R	$E_1 = \infty \cdot GPa$, $\nu_1 = 0$	-
body 2	Half-space $R = \infty \cdot m$	EP	$E_2 = 210GPa$, $\nu_2 = 0.3$	Swift's law with $B_2 = 945MPa$, $C_2 = 20$, $n_2 = 0.121$

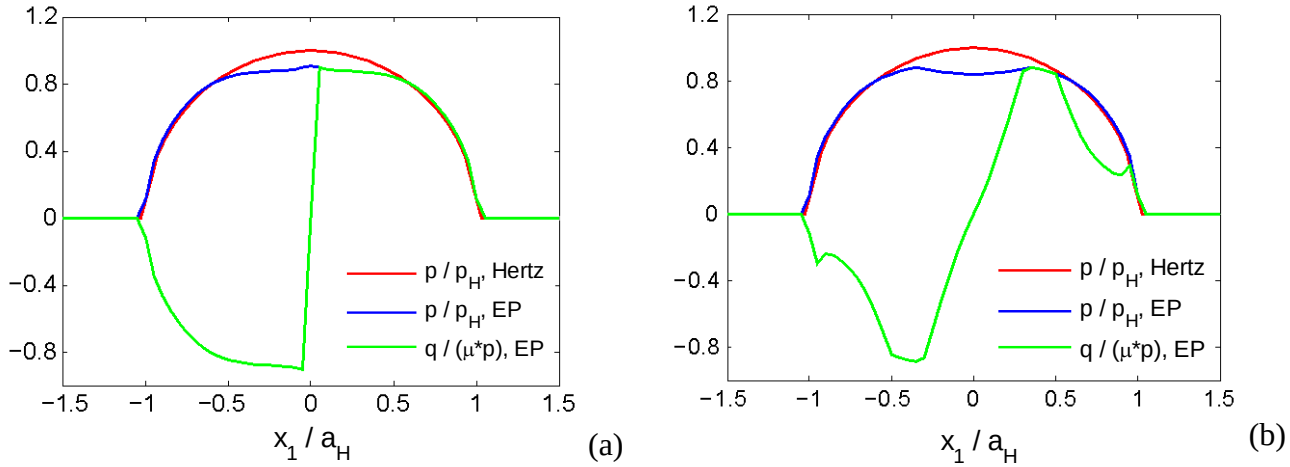

Fig. 5. Profiles of dimensionless contact tractions (p is the contact pressure and $q=\sqrt{q_1^2+q_2^2}$ the shear traction): a) $\mu=0.1$; b) $\mu=0.2$;

Figure 5(a) exhibits a stick central region and a slip annulus as in the case of the purely elastic contact, i.e. as in the classical solution of Cattaneo-Mindlin. For a 0.2 frictional coefficient, as shown in fig. 5(b), two regions of slip and two of stick are predicted. Further increase of the frictional coefficient results in highly irregular shear stresses and multiple annuli of alternating slip and stick. One can question if the imposed spatial or load application resolution is high enough as to replicate such complicated behaviour.

The influence of the frictional coefficient on the development of plastic strains is depicted in figure 6. The maximum plastic strains are indicated on each plot. One can see that, with more intense frictional regimes, the plastic strains volume advances toward the free surface. Figure 6(d) shows that the maximum plastic strain reaches 2%, which is established in the literature as the limit of small plastic deformations, and thus further loading does not obey the framework of small deformations. A comparison between figures 6(a) - frictionless contact, and 5(d) proves that, when friction is neglected, the maximum plastic strain is underestimated by nearly 40%.

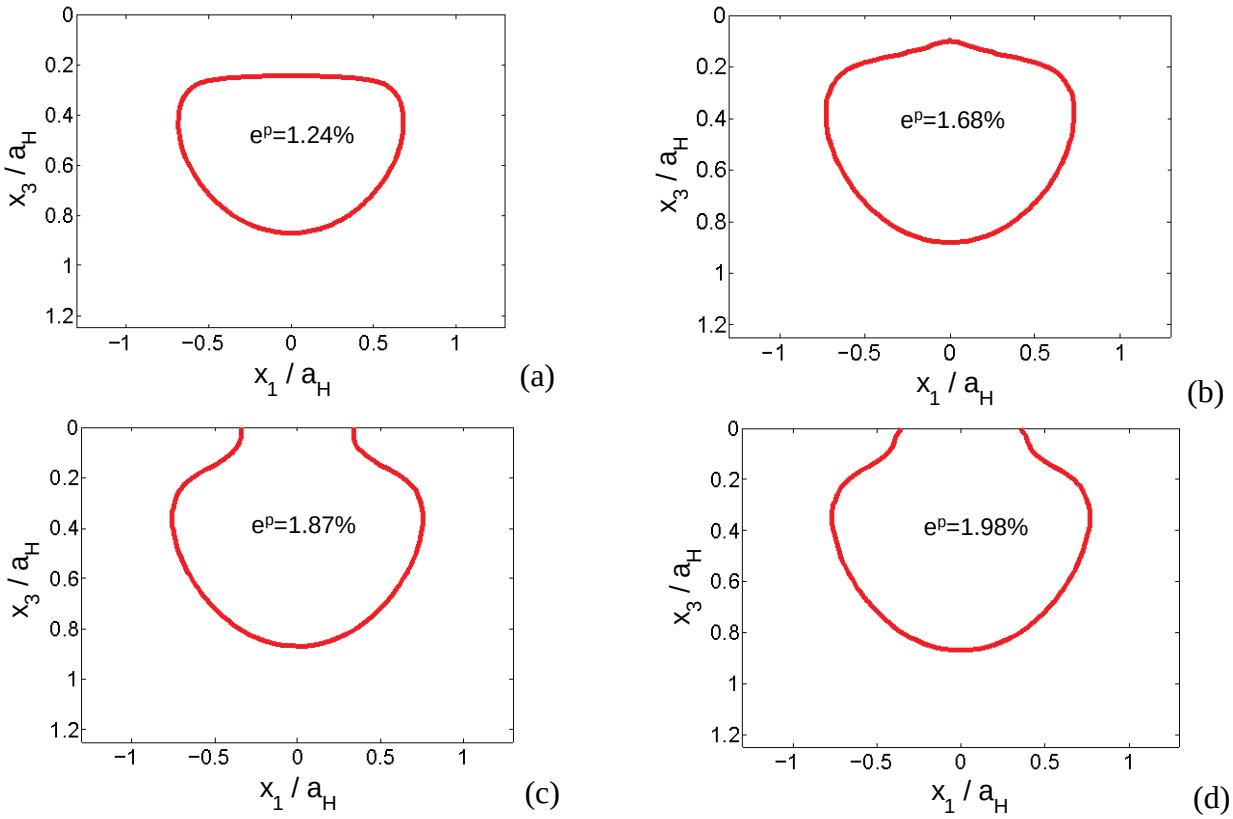

Fig. 6. Influence of the frictional regime on the extent of the plastic strain volume: a) $\mu=0$ (frictionless), b) $\mu=0.1$; c) $\mu=0.2$; d) $\mu=0.5$

5. CONCLUSIONS

This paper improves an existing computer code for the numerical simulation of the elastic-plastic contact problem by adding the influence of friction. The one level elastic loop in the original algorithm, accomplishing the solution of the frictionless contact problem, is substituted by a two-level nested loop, in which the solutions of the normal and of the tangential contact problems are successively obtained until convergence. The result is an algorithm based on four levels of iterations capable of describing an elastic contact process under slip and stick conditions. The new approach is supported by recent results obtained by the same author concerning the tangential residual displacements induced by arbitrary distributions of plastic strains.

The frictional contact with geometric symmetry and similar elastic-plastic behaviour of the contacting materials is simulated with the new model, and a new interference equation is derived that bypasses the slip-stick loop.

Results for the slip-stick indentation of an elastic-plastic half-space by a rigid spherical indenter are presented for various frictional coefficients. The numerical simulations suggest that multiple regions of stick and slip develop in a fretting process of type II. The influence of the frictional coefficients on the extents of the volume with plastic strains is depicted. Compared to the frictionless contact, the plastic region advances toward the free surface on the contact axis. For a frictional coefficient of 0.5, the maximum plastic strain is under evaluated by nearly 40% when the frictionless contact model is applied to the same contact scenario.

Highly irregular profiles of contact tractions were predicted for intense frictional regimes, suggesting that higher resolutions for both spatial discretisation and loading history reproduction, may be required to achieve well-converged solutions.

Conflicts of Interest: There is no conflict of interest.

6. REFERENCES

1. Johnson, K. L., (1985). Contact Mechanics (Cambridge: University Press).
2. Brizmer, V., Zait, Y., Kligerman, Y., and Etsion, I., (2006). *The Effect of Contact Conditions and Material Properties on Elastic-Plastic Spherical Contact,* Journal of Mechanics of Materials and Structures, 1(5), 865-879.
3. Zait, Y., Kligerman, Y., Etsion, I., (2010). *Unloading of an Elastic-Plastic Spherical Contact under Stick Contact Condition,* International Journal of Solids And Structures, 47(7-8) 990-997.
4. Jacq, C., Nelias, D., Lormand, G., Girodin, D., (2002). *Development of a Three-Dimensional Semi-Analytical Elastic-Plastic Contact Code*, ASME Journal of Tribology, 124, 653-667.
5. Wang, F., Keer, L. M., (2005). *Numerical Simulation for Three Dimensional Elastic-Plastic Contact with Hardening Behavior*, ASME Journal of Tribology, 127, 494-502.
6. Nélias, D., Boucly, V., and Brunet, M., (2006). *Elastic-Plastic Contact Between Rough Surfaces: Proposal for a Wear or Running-in Model*, ASME J. Tribol., 128, 236 - 244.
7. Chen, W. W., Liu, S., Wang, Q. J., (2008). *Fast Fourier Transform Based Numerical Methods for Elasto-Plastic Contacts of Nominally Flat Surfaces*, ASME J. Tribol., 75, 011022.
8. Chaise, T., Nélias, D., (2011). *Contact Pressure and Residual Strain in 3D Elasto-Plastic Rolling Contact for a Circular or Elliptical Point Contact*, ASME J. Tribol., 133, 041402.
9. Boucly, V., Nélias, D., and Green, I., (2007). *Modeling of the Rolling and Sliding Contact Between Two Asperities* ASME J. Tribol., 129, 235 – 245.
10. Nélias, D., Antaluca, E., Boucly, V., and Crețu, S., (2007). *A Three-Dimensional Semianalytical Model for Elastic-Plastic Sliding Contacts*, ASME J. Tribol., 129, 761 – 771.
11. Chen, W. W., Wang, Q. J., Wang, F., Keer, L. M., and Cao, J., (2008). *Three-Dimensional Repeated Elasto-Plastic Point Contacts, Rolling, and Sliding*, ASME J. Tribol., 75, 021021.
12. Wang, Z., Jin, X., Liu, S., Keer, L. M., Cao, J., and Wang, Q., (2013). *A New Fast Method for Solving Contact Plasticity and its Application in Analyzing Elasto-Plastic Partial Slip*, Mechanics of Materials, 60, 18-35.
13. Cerlinca, D., Spinu, S., (2022), *Numerical Simulation of Elastic-Plastic Contact with Isotropic Hardening*, International Journal of Modern Manufacturing Technologies, 14(2), 294 – 301.
14. Spinu, S., (2024), *Residual Displacement due to Arbitrary Plastic Strains*, accepted for publication in International Journal of Modern Manufacturing Technologies, XVI (3).
15. Spinu S., Amarandei D., (2012), *Numerical Simulation of Slip-Stick Elastic Contact*, In: Numerical Simulation - From Theory to Industry, pp. 129-154, Mykhaylo Andriychuk (Ed), InTech, ISBN 978-953-51-0749-1.

Received: March 18, 2024 / Accepted: June 15, 2024 / Paper available online: June 20, 2024